

ORIGINAL ARTICLE

Validation of real-time prostatic biopsies evaluation with fluorescence laser confocal microscopy

Stefano GOBBO ^{1, 2} *, Albino ECCHER ³, Sebastian GALLINA ⁴, Damiano D'AIETTI ⁴,
Alessandro PRINCIOTTA ⁴, Francesco DITONNO ⁴, Alessandro TAFURI ⁴,
Maria A. CERRUTO ⁴, Stefano MARLETTA ^{2, 5}, Francesca SANGUEDOLCE ⁶,
Aldo SCARPA ², Matteo BRUNELLI ², Alessandro ANTONELLI ⁴

¹Department of Translational Medicine, University of Ferrara, Ferrara, Italy; ²Section of Pathology, Department of Diagnostic and Public Health, University of Verona, Verona, Italy; ³Department of Pathology and Diagnostics, University and Hospital Trust of Verona, Verona, Italy; ⁴Department of Urology, University Hospital of Verona, University of Verona, Verona, Italy; ⁵Unit of Pathology, Pederzoli Hospital, Peschiera del Garda, Verona, Italy; ⁶Unit of Pathology, Ospedali Riuniti University Hospital, University of Foggia, Foggia, Italy

*Corresponding author: Stefano Gobbo, Department of Translational Medicine, University of Ferrara, Via Luigi Borsari, 46, 44121 Ferrara, Italy. E-mail: gbbssf@unife.it

ABSTRACT

BACKGROUND: Routine processing of prostate biopsies requires conventional steps that usually take a few days. The aim of this study was to validate the use of fluorescence laser confocal microscopy (FCM) for real-time diagnostics.

METHODS: We prospectively tested images from prostate needle biopsies (75 images were evaluated by FCM and conventional slides). Two pathologists reviewed the images and assessed agreements between FCM *versus* conventional slides and between pathologists (κ -values). Interpretation was performed on digital images from the VivaScope 2500 confocal microscope (MAVIG GmbH, Munich, Germany; Caliber I.D., Rochester, NY, USA) placed in the urological operating room. Cancerous *versus* benign tissue was the primary focus, then the application of the grading system.

RESULTS: Cancer was diagnosed in 24 conventional slides (on 75 images) in which agreement among pathologists was high for both conventional ($\kappa=0.96$) and FCM ($\kappa=0.84$). 1/24 (4%) was ISUP/WHO grade group I, 12/24 (50%) II, 8/24 (33%) III, 2/24 (8%) IV and 1/24 (4%) grade V. Near perfect agreement was obtained for grades I, IV and V ($\kappa=0.85$). Grade III values achieved a moderate agreement ($\kappa=0.55$). The mean time for laser scanning was 9 minutes. For the remaining non-tumor images, agreement was nearly perfect ($\kappa=0.81$).

CONCLUSIONS: We validated the use of FCM for real-time cancer detection in prostate biopsies.

(Cite this article as: Gobbo S, Eccher A, Gallina S, D'Aietti D, Princiotta A, Ditunno F, *et al.* Validation of real-time prostatic biopsies evaluation with fluorescence laser confocal microscopy. *Minerva Urol Nephrol* 2023;75:577-82. DOI: 10.23736/S2724-6051.23.05352-1)

KEY WORDS: Prostatic neoplasms; Microscopy, fluorescence, multiphoton; Pathology; Diagnostic techniques, urological.

Prostate cancer is the most frequent malignancy in male subjects.¹ Early diagnosis is mandatory for better patient management and histopathology analysis of prostate biopsies is the gold standard in timely diagnosis.^{2, 3} Histopathology of prostate biopsies requires a time-consuming approach, including fixation of specimens, paraffin embedding, and slide production consisting of routine steps that usually take a few days. The

application of *ex-vivo* fluorescence confocal microscopy (FCM) on prostate biopsies was evaluated to make possible a real-time histopathological diagnosis.⁴ Confocal microscopy is an optical imaging technique that uses a laser that generates fluorescence or reflectance from the focal point. Produces digital images similar to conventional histopathology slides by computationally recreating H&E-like images ready to use for histopa-

thology analyses.⁵ In 2019, Puliatti *et al.* evaluated this approach by analyzing 89 prostate biopsy images taken with an 18G biopsy punch on the fresh surgical specimen at the end of 13 prostatectomies. They obtained a substantial overall diagnostic agreement between FCM and conventional histopathological diagnoses with 91% correct diagnosis ($\kappa=0.75$).⁴ In 2020, Marengo *et al.* analyzed 182 FCM images from 65 regions of interest (ROI) on 57 patients undergoing prostate biopsies. They reported a median time to acquisition of 5 minutes. The endpoint was to evaluate the agreement between FCM and conventional histopathologic analysis in detecting neoplastic tissue.⁶ In 2021, Rocco *et al.* analyzed 427 FCM images from 54 patients considering the agreement with the analysis of digital slides from conventional histological preparations in the detection of prostate cancer by 4 expert pathologists. Their second objective was also to evaluate the agreement in the classification of prostate cancer sec. ISUP.⁷ These pioneering experiments and the subsequent review by Rocco *et al.* underlined the promising value of FCM in real-time detection of prostate cancer from biopsies arguing the need to validate the use of this technology by expanding the experience with more cases and from different uropathology centers.⁸ In our study we reproduced the same experiment on consecutive cases in the urology center of the University of Verona considering the same endpoints to validate the results. Another aim of our study was to evaluate the perceived usability of the FCM system. The subjective component of perceived usability, in addition to the objective efficiency and effectiveness, constitutes the classical conception of the construct of usability, fundamental for the user experience.

Materials and methods

We set up an FCM instrument (VivaScope 2500 Confocal Microscope; MAVIG GmbH, Munich, Germany; Caliber I.D., Rochester, NY, USA) in the urological operating room of the University of Verona for three months (from July 2021 to September 2021). For each prostate biopsy sample, we tested the real-time approach directly in the operating room. The VivaScope 2500M-G4

FCM (MAVIG GmbH; Caliber I.D.) analyzes the reflectance (785 nm) and fluorescence (488 nm) of two different lasers enabling tissue morphological examination. The maximum total scan area is 25×25 mm reaching a magnification of ×550.⁹ Histological images were generated by company software, VivaScan® (version 11.0.1140 MAVIG GmbH; Caliber I.D.), VivaBlock® and VivaStack® to convert the grayscale mosaics into H&E-like digitally colored images. After acquisition of the FCM images, the stained samples were fixed in formalin and sent to routine processing in the pathology department of the University of Verona for conventional histopathological analyzes. Two pathologists attended a short one-day course for the presentation of the specific technical properties of FCM increasing their confidence with the FCM images by analyzing about 30 cases of different tissue samples proposed by the product specialist. In our institution we started early with the experience of prostate biopsies with a rapid learning curve. These two expert uropathologists examined the H&E-like digital images obtained from the FCM trying to detect neoplastic tissue. They were called to answer if positive or negative for tumor, when the interpretation was equivocal the histopathological report remained pending. The same pathologists analyzed the corresponding randomly placed conventional slides blindly after a few days.

Statistical analysis

We assessed agreements between FCM diagnostics *versus* standard slides and between pathologists (κ -values). The presence of cancerous tissue *versus* benign tissue was the main focus, hence the application of the classification systems (sec. ISUP/WHO) applied after cancer detection.¹⁰ Agreement between the FCM and conventional histopathologic diagnoses was expressed using Cohen's κ statistic. Furthermore, inter-observer agreement was assessed for both FCM evaluation and conventional histopathological diagnosis.

Results

Overall, we tested 75 digital images and the corresponding conventional slides (Table I). Sixty-

TABLE I.—*Diagnosis for each case on conventional glass slides compared with diagnosis on H&E-like digital images from fluorescence confocal microscopy.*

N. images	Diagnosis at conventional glass slides	Diagnosis at H&E-like images (from FCM)	Origin of tissue	Gleason Score and grading groups (sec. ISUP)
1	Adenocarcinoma	Adenocarcinoma	Biopsy	4+4, IV
2	Adenocarcinoma	Adenocarcinoma	Biopsy	3+4, II
3	Adenocarcinoma	Adenocarcinoma	Biopsy	3+4, II
4	Adenocarcinoma	Adenocarcinoma	Biopsy	4+4, IV
5	Adenocarcinoma	Adenocarcinoma	Biopsy	3+4, II
6	Adenocarcinoma	Adenocarcinoma	Biopsy	4+4, IV
7	Adenocarcinoma	Adenocarcinoma	Biopsy	4+3, III
8	Adenocarcinoma	Adenocarcinoma	Biopsy	4+5, V
9	Adenocarcinoma	Adenocarcinoma	Biopsy	3+4, II
10	Adenocarcinoma	Adenocarcinoma	Biopsy	3+4, II
11	Adenocarcinoma	Adenocarcinoma	Biopsy	3+4, II
12	Adenocarcinoma	Adenocarcinoma	Biopsy	3+4, II
13	Adenocarcinoma	Adenocarcinoma	Biopsy	3+4, II
14	Adenocarcinoma	Adenocarcinoma	Biopsy	4+3, III
15	Adenocarcinoma	Adenocarcinoma	Biopsy	4+3, III
16	Adenocarcinoma	Adenocarcinoma	Biopsy	4+3, III
17	Adenocarcinoma	Adenocarcinoma	Prostatectomy	3+4, II
18	Adenocarcinoma	Adenocarcinoma	Prostatectomy	4+3, III
19	Adenocarcinoma	Adenocarcinoma	Prostatectomy	4+3, III
20	Adenocarcinoma	Adenocarcinoma	Prostate transplantation	3+4, II
21	Adenocarcinoma	Adenocarcinoma	Prostate transplantation	4+4, IV
22	Adenocarcinoma	Pending evaluation	Prostate transplantation	3+4, II
23	Adenocarcinoma	Pending evaluation	Biopsy	3+4, II
24	Adenocarcinoma	Pending evaluation	Biopsy	3+3, I
25	Benign tissue	Pending evaluation	Biopsy	N.a.
26	Benign tissue	Pending evaluation	Biopsy	N.a.
27	Benign tissue	Pending evaluation	Biopsy	N.a.
28	Benign tissue	Pending evaluation	Biopsy	N.a.
29	Benign tissue	Pending evaluation	Biopsy	N.a.
30	Benign tissue	Pending evaluation	Biopsy	N.a.
31	Benign tissue	Pending evaluation	Biopsy	N.a.
32	Benign tissue	Pending evaluation	Biopsy	N.a.
33	Benign tissue	Benign	Biopsy	N.a.
34	Benign tissue	Benign	Biopsy	N.a.
35	Benign tissue	Benign	Biopsy	N.a.
36	Benign tissue	Benign	Biopsy	N.a.
37	Benign tissue	Benign	Biopsy	N.a.
38	Benign tissue	Benign	Biopsy	N.a.
39	Benign tissue	Benign	Biopsy	N.a.
40	Benign tissue	Benign	Biopsy	N.a.
41	Benign tissue	Benign	Biopsy	N.a.
42	Benign tissue	Benign	Biopsy	N.a.
43	Benign tissue	Benign	Biopsy	N.a.
44	Benign tissue	Benign	Biopsy	N.a.
45	Benign tissue	Benign	Biopsy	N.a.
46	Benign tissue	Benign	Biopsy	N.a.
47	Benign tissue	Benign	Biopsy	N.a.
48	Benign tissue	Benign	Biopsy	N.a.
49	Benign tissue	Benign	Biopsy	N.a.
50	Benign tissue	Benign	Biopsy	N.a.
51	Benign tissue	Benign	Biopsy	N.a.
52	Benign tissue	Benign	Biopsy	N.a.
53	Benign tissue	Benign	Biopsy	N.a.
54	Benign tissue	Benign	Biopsy	N.a.
55	Benign tissue	Benign	Biopsy	N.a.
56	Benign tissue	Benign	Biopsy	N.a.

(To be continued)

This document is protected by international copyright laws. No additional reproduction is authorized. It is permitted for personal use to download and save only one file and print only one copy of this Article. It is not permitted to make additional copies (either sporadically or systematically, either printed or electronic) of the Article for any purpose. It is not permitted to distribute the electronic copy of the article through online internet and/or intranet file sharing systems, electronic mailing or any other means which may allow access to the Article. The use of all or any part of the Article for any Commercial Use is not permitted. The production of derivative works from the Article is not permitted. It is not permitted to remove, cover, overlay, obscure, block, or change any copyright notices or terms of use which the Publisher may post on the Article. It is not permitted to frame or use framing techniques to enclose any trademark, logo, or other proprietary information of the Publisher.

TABLE I.—*Diagnosis for each case on conventional glass slides compared with diagnosis on H&E-like digital images from fluorescence confocal microscopy (continues).*

N. images	Diagnosis at conventional glass slides	Diagnosis at H&E-like images (from FCM)	Origin of tissue	Gleason Score and grading groups (sec. ISUP)
57	Benign tissue	Benign	Biopsy	N.a.
58	Benign tissue	Benign	Biopsy	N.a.
59	Benign tissue	Benign	Biopsy	N.a.
60	Benign tissue	Benign	Biopsy	N.a.
61	Benign tissue	Benign	Biopsy	N.a.
62	Benign tissue	Benign	Biopsy	N.a.
63	Benign tissue	Benign	Biopsy	N.a.
64	Benign tissue	Benign	Biopsy	N.a.
65	Benign tissue	Benign	Biopsy	N.a.
66	Benign tissue	Benign	Biopsy	N.a.
67	Benign tissue	Benign	Biopsy	N.a.
68	Benign tissue	Benign	Biopsy	N.a.
69	Benign tissue	Benign	Biopsy	N.a.
70	Benign tissue	Benign	Biopsy	N.a.
71	Benign tissue	Benign	Biopsy	N.a.
72	Benign tissue	Benign	Biopsy	N.a.
73	Benign tissue	Benign	Biopsy	N.a.
74	Benign tissue	Benign	Biopsy	N.a.
75	Benign tissue	Benign	Biopsy	N.a.

FCM: fluorescence confocal microscopy; N.a.: not applicable.

nine specimens from 20 patients undergoing prostate biopsies, 3 biopsies performed from the bench on a prostatectomy specimen, and 3 from a transplant donor prostate. The pathologists were confident in the report in 64 cases (85%), in the remaining 11 cases (15%) the interpretation was considered equivocal and preferred to defer the diagnosis to conventional slide analysis. Two cases were considered equivocal because the FCM digital image generated by the instrument was fuzzy and distorted, unusable for correct interpretation. Nine cases were considered equivocal due to the pathologist's lack of confidence in tissue interpretation, especially in low-grade tumors (3 cases) and in normal prostate tissue particularly crowded with glands. In low-grade prostate cancer, the need for immunohistochemistry to confirm the missing basal layer has made interpretation deferrable requiring conventional processing. Cancer was detected in 24 conventional histopathology slides by both pathologists with near-perfect agreement between pathologists for both conventional and H&E-like slides from FCM; the agreement was (0.96 for HE, $\kappa=0.96$; 0.95 for FCM, $\kappa=0.84$). In these 24 cancer cases, only 3 analyzed images on H&E-like slides from FCM were equivocal with pending evaluation. In 9 cases pathologists were

confident of reporting benign cancer-negative tissue with perfect agreement with the diagnosis on conventional slides. Of the 11 pending cases, 3 (27%) were later diagnosed cancer positive and 8 resulted as cancer negative. Low agreement was obtained in the evaluation of inflammatory tissue on non-cancerous and cancerous tissues ($\kappa=0.22$). Regarding the application of the classification system according to ISUP, the detected neoplastic tissue was 1/24 (4%) grade group I, 12/24 (50%) grade group II, 8/24 (33%) grade group III, 2/24 (8%) grade group IV, and 1/24 (4%) grade group V. Agreement for grade groups I, IV, and V between FCM digital images and conventional slides was high ($\kappa=0.85$). Values for grade groups II-III reached high agreements taken together ($\kappa=0.62$), moderate for grade group III individually ($\kappa=0.55$). The time for the laser scan ranged from 7 minutes to 14 minutes (average 9 minutes).

Discussion

We have extended the series of prostate biopsies analyzed with FCM digital images trying to validate this method and its utility in a promising real-time evaluation for immediate patient counseling in the urological surgical room. In the

detection of prostate cancer tissue, the agreement between results obtained from H&E-like digital images from FCM and conventional H&E slides analyzed by light microscope was perfect when equivocal cases were excluded. Since the aim of our experiment was to provide an accurate evaluation in real-time for appropriate counseling to the patient, in the 11 equivocal cases it was preferred to suspend the evaluation rather than risk an unsure diagnosis. All cases diagnosed positive for cancer on FCM images (21 cases) were confirmed positive on conventional slides. In addition, all the images considered negative for neoplasia on FMC analysis were ultimately confirmed as negative on conventional microscopic evaluation demonstrating perfect agreement in the diagnosis of benign prostatic tissue. These results confer high specificity and sensitivity of FCM in prostatic cancer detection without false positive and false negative images (Figure 1). In previous studies, the agreement between the diagnosis on H&E-like digital images and conventional H&E slides for prostatic biopsies was very high (Puliatti, $\kappa=0,75$; Marengo, $\kappa=0,81$; Rocco, $\kappa=0,84$).^{4, 6, 7} Considering all samples tested in these studies together with our samples (total of

762 images), the mean agreement expressed in Cohen's κ is 0.85. Regarding our second endpoint, concerning the application of the ISUP grading system, the agreement between FCM and conventional slides was higher for extreme grade groups I, IV and V ($\kappa=0.85$). For the grade groups II (Gleason Score 3+4) and III (Gleason Score 4+3) which are sometimes critical for differentiating between a radical prostatectomy or a wait-and-see approach, agreement was not satisfactory ($\kappa=0.62$). Lack of confidence in identifying the proper proportion of Gleason patterns 3 and 4 on FCM digital images has made it difficult to choose between these two groups of ISUP grade groups. This observation advises against the use of FMC in prostate cancer classification, even considering that it would probably not be crucial in the need for timely patient counseling. In addition, 3 of the 11 equivocal cases were ultimately diagnosed as positive for grade I or II prostate cancer, indicating greater difficulty in detecting low-grade malignancy. Furthermore, this early approach to detecting cancer on FMC digital images could be very useful in the evaluation of suspected malignancy in a transplanted organ donor. In short, after all these considerations, in order to provide adequate patient counseling, the pathologist should be confident in the real-time evaluation of prostate biopsies with FMC imaging in negative cases and in positive cases with a high-grade malignancy. The suggestion is to suspend reporting in all equivocal cases including suspicion of low-grade malignancy that need to be confirmed by conventional microscopic analysis.

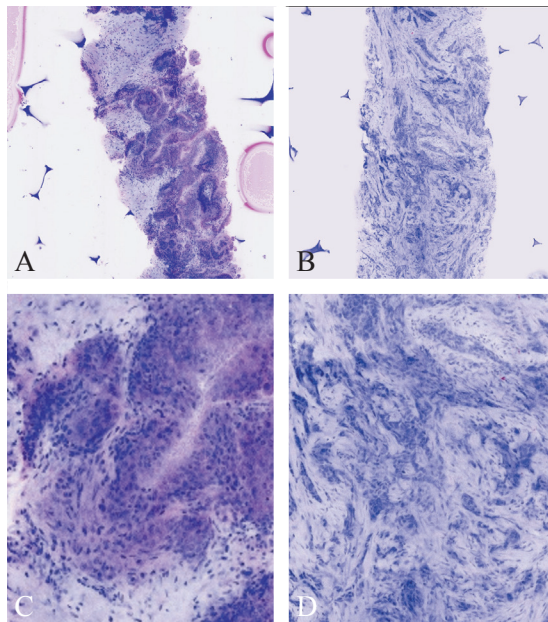


Figure 1.—Digital images from fluorescence confocal microscopy: A, C) normal prostatic tissue; and B, D) prostatic adenocarcinoma.

Conclusions

In conclusion, these results validate the usefulness of the FMC system in real-time detection of cancer in prostatic biopsies making it considered a valid aid for the pathologists involved in consulting the patient allowing a rapid organization of the diagnostic-therapeutic pathway.

References

1. Sung H, Ferlay J, Siegel RL, Laversanne M, Soerjomataram I, Jemal A, *et al.* Global Cancer Statistics 2020: GLOBO-

CAN Estimates of Incidence and Mortality Worldwide for 36 Cancers in 185 Countries. *CA Cancer J Clin* 2021;71:209–49.

2. Lomas DJ, Ahmed HU. All change in the prostate cancer diagnostic pathway. *Nat Rev Clin Oncol* 2020;17:372–81.

3. Connor MJ, Gorin MA, Eldred-Evans D, Bass EJ, Desai A, Dudderidge T, *et al.* Landmarks in the evolution of prostate biopsy. *Nat Rev Urol* 2023;20:241–58.

4. Puliatti S, Bertoni L, Pirola GM, Azzoni P, Bevilacqua L, Eissa A, *et al.* Ex vivo fluorescence confocal microscopy: the first application for real-time pathological examination of prostatic tissue. *BJU Int* 2019;124:469–76.

5. Bayguinov PO, Oakley DM, Shih CC, Geanon DJ, Joens MS, Fitzpatrick JA. Modern Laser Scanning Confocal Microscopy. *Curr Protoc Cytom* 2018;85:e39.

6. Marengo J, Calatrava A, Casanova J, Claps F, Mascaros J, Wong A, *et al.* Evaluation of Fluorescent Confocal Microscopy for Intraoperative Analysis of Prostate Biopsy Cores. *Eur Urol Focus* 2021;7:1254–9.

7. Rocco B, Sighinolfi MC, Sandri M, Spandri V, Cimadamore A, Volavsek M, *et al.* Digital Biopsy with Fluorescence Confocal Microscope for Effective Real-time Diagnosis of Prostate Cancer: A Prospective, Comparative Study. *Eur Urol Oncol* 2021;4:784–91.

8. Rocco B, Cimadamore A, Sarchi L, Bonetti LR, Bertoni L, Azzoni P, *et al.* Current and future perspectives of digital microscopy with fluorescence confocal microscope for prostate tissue interpretation: a narrative review. *Transl Androl Urol* 2021;10:1569–80.

9. Vivascope. MAVIG GmbH. MAVIG VivaScope – Technical Data; 2019 [Internet]. Available from: <http://www.vivascope.de/en/products/devices/ex-vivo-devices/vivascope-2500-multilaser/technical-data.html> [cited 2023, Jun 29].

10. van Leenders GJ, van der Kwast TH, Grignon DJ, Evans AJ, Kristiansen G, Kweldam CF, *et al.*; ISUP Grading Workshop Panel Members. The 2019 International Society of Urological Pathology (ISUP) Consensus Conference on Grading of Prostatic Carcinoma. *Am J Surg Pathol* 2020;44:e87–99.

Conflicts of interest

The authors certify that there is no conflict of interest with any financial organization regarding the material discussed in the manuscript.

Authors' contributions

All authors read and approved the final version of the manuscript.

History

Article first published online: July 24, 2023. - Manuscript accepted: June 26, 2023. - Manuscript revised: June 8, 2023. - Manuscript received: March 16, 2023.